

Available at www.sciencedirect.com

SciVerse ScienceDirect

journal homepage: www.elsevier.com/locate/carbon

Selective etching of armchair edges in graphite

G. Dobrik^{*}, L. Tapasztó, L.P. Biró

Institute of Technical Physics and Materials Science, Research Centre for Natural Sciences, P.O. Box 49, H-1525 Budapest, Hungary

ARTICLE INFO

Article history:

Received 19 September 2012

Accepted 11 January 2013

Available online 22 January 2013

ABSTRACT

We present an easy and fast procedure for producing graphene and few layer graphite nanostructures with edges of predefined crystallographic orientation. By annealing graphite in an oxygen containing atmosphere, of controlled composition hexagonal surface structures can be etched in a controlled way. We show that the process can be made crystallographically selective and the resulting edges are of armchair type. The dimensions of the resulting nanostructures can be well controlled by the oxidation rate, through accurately adjusting the etching parameters, such as oxygen concentration, annealing temperature and duration. The oxidation preferentially starts at defect sites either naturally present in the sample or produced on purpose, the latter holding the promise of a more accurate control over the resulting structures.

© 2013 Elsevier Ltd. All rights reserved.

1. Introduction

Graphene – a single atomic layer of graphite – is in the focus of intense research efforts since its discovery [1]. Several production methods have been developed thus far, but the best quality samples are still produced by mechanical exfoliation [1]. CVD growth of graphene on Ni [2] or Ni thin films are also promising ways of producing large area, high quality sheets, along with metals like Ru, Cu [3] or even highly oriented pyrolytic graphite (HOPG) used for graphene epitaxy [4]. Epitaxial growth of graphene on SiC is also a well-established method [5]. There are a variety of methods of chemical exfoliation [6], including the ones using organic solvents to enhance exfoliation [7].

Due to its high electron mobility and long coherence length [8], graphene attracts an increasing interest as a promising new material for next-generation electronic devices [9]. However, a major drawback for mainstream logic applications is that graphene remains metallic even at the charge neutrality point. The production of graphene nanoribbons (GNRs) with well controlled crystallographic orientation and atomically precise edges is considered to be the most straightforward way to open a gap in the electronic structure of

graphene. Theoretical studies predicted that this gap strongly depends on both the width and crystallographic orientation of GNRs. The largest band gap can be achieved for narrow armchair-edged ribbons [10]. A deviation of a few degrees from the armchair crystallographic orientation can drastically decrease the size of the band gap. Therefore, if nanoelectronic applications are envisaged, experimental methods producing graphene nanostructures with precisely armchair orientations are of particular importance [10,11].

To date, the standard lithographic procedures like e-beam lithography are unable to accomplish the required accuracy in the control of the crystallographic orientation and width of graphene nanoribbon (GNR) in the nanometer range [12]. The width of GNRs produced by anodic oxidation under the AFM tip, seems also to be limited in the range of few tens of nanometers, and no crystallographic orientation control is provided [13]. One of the techniques able to achieve simultaneously the crystallographic orientation and the size control of GNRs of nanometer widths is scanning tunneling lithography [14]. Other methods possibly offering crystallographic orientation control of the etched GNRs, or other nanopatterns, can be divided in two categories: (i) methods based on nanoparticle induced patterning [15], (ii) methods based

^{*} Corresponding author.

on controlled oxidation or controlled hydrogen plasma etching [16]. The latter methods rely on the selective chemical reaction for the removal of C atoms from the edge of the graphene sheet, therefore the crystallographic control is related to the different reaction rates of C atoms in zig-zag, or armchair positions. In the case of patterns etched by mobile nanoparticles it is a serious drawback that the starting point and etching direction cannot be easily controlled. Etching of variously shaped pits in the surface of HOPG by oxidation in air has also been reported before [17–19].

In this paper we propose a simple method for producing highly regular hexagonal holes with precisely armchair oriented edges in graphite, then we exfoliate them into patterned graphene and few layer graphite flakes. Our method is based on the crystallographically selective oxidation of graphitic layers in controlled, oxygen containing atmosphere.

2. Experimental results and discussion

Highly oriented pyrolytic graphite (HOPG SPI-1 from SPI) samples were used in our experiments. For each experiment freshly cleaved HOPG surfaces have been used. The sample was placed in a quartz tube located in a resistively heated furnace. The temperatures used were typically between 300 and 800 °C. An oxygen/inert gas mixture (0–45% oxygen) was flowing at slightly larger pressure than the atmospheric pressure through the quartz tube. During the experiment, first, the sample was heated up in an inert gas environment. After the sample reached the desired temperature (with a heating rate of about 50 °C/min), the desired concentration of oxygen gas was added to the inert gas. After the heat treatment, the sample was cooled down quickly in an inert atmosphere (with a cooling rate of 50 °C/s). The duration of oxidation time ranged between 5 and 20 min. The resulting samples were investigated by Atomic Force Microscopy (AFM) and Scanning Tunneling Microscopy (STM) using a commercial Nanoscope III Multimode AFM/STM instrument.

When HOPG samples are heated up to about 600 °C in oxygen containing atmosphere the etching of their surface occurs. Such an etched surface can be seen in Fig. 1. The surface exhibits two types of characteristic topographic features: (i) randomly curved and branching trenches, and (ii) hexagonal holes of very regular shape. The first type features originate from etched grain boundaries (GB) [20] while the second type features most probably originate from point-like native defects (e.g., vacancies or dislocation lines perpendicular to the surface). The hexagonal holes can be characterized well by their average diameter. It is worth noting that the etched grain boundaries are present in form of several micron long straight segments, as marked by the white arrows in Fig. 1. The angle values in the inset of Fig. 1, (representing the angles between different HOPG grains) indicate the edge selectivity of the etching process. In Fig. 1 two groups of hexagonal holes with different orientation can be identified, marked by (blue (B) and red ovals (A)). They correspond to two distinct graphite crystallites, which are rotated relative to each other. The two larger crystal grains (A and B) are separated by a broad, well etched grain boundary and a small crystallite (C) intercalated between them. One can observe

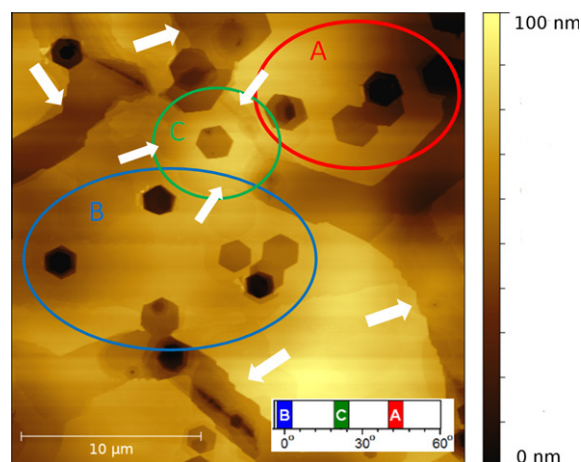


Fig. 1 – AFM image of the etched HOPG surface. The surface exhibits two types of characteristic features: wide trenches (marked by white arrows) and hexagonal holes (marked by colored ovals). Inset: representing the angles between different HOPG grains (A–C). (For interpretation of the references to color in this figure legend, the reader is referred to the web version of this article.)

in Fig. 1 that the hexagonal hole in crystallite C has an intermediate orientation between those in crystallite A and B. The grain boundary between A and C was etched to a much smaller extent than the grain boundary between A and B. On the other hand the grain boundary between B and C is barely visible. This shows that under the etching conditions used, it is possible to a certain degree to discriminate between different types of grain boundaries. The difference in the etching behavior of grain boundaries may be associated with their different crystallographic structure. A strongly disordered GB, like that calculated for graphene layers in Ref. [21] very likely will be subjected to a strong oxidation, while a more regular kind of GB like those reported in [22,23] will be less prone to intensive oxidation.

Oxidation of graphite starts much easier at defect sites because the in-plane carbon–carbon covalent bonds in graphene are very stable [24]. Therefore, the dangling bonds present at any defect site offer a facile attack point for oxidation. HOPG is a mosaic crystal, which depending on the quality of the material is composed of grains of several microns in width and a few tens to hundreds of nanometers in thickness. These grains are arranged in a way that their “c” axis point with a small deviation in the same direction. Fig. 2 shows a schematic presentation of the different oxidation processes that have been observed in our STM investigations. In Fig. 2a the oxidation of a point defect versus the oxidation of a grain boundary is shown schematically. In the region of the large angle grain boundary, where the mismatch of the two neighboring lattices cannot be accommodated by the incorporation of nonhexagonal rings into the graphene, the oxygen may penetrate deep into the material by diffusion. The diffusion along defects is much faster than the bulk diffusion [25]. If the diffusion rate is much larger than the oxidation speed, the walls of the etched feature will be close to the perpendicular to the sample surface. This will lead to the

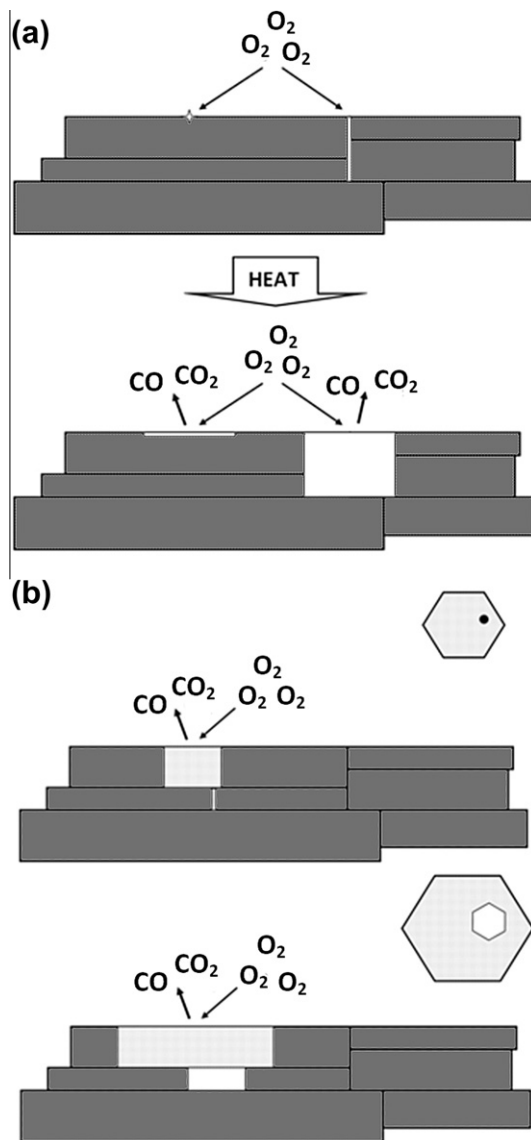


Fig. 2 – Schematic figure of the etching process. (a) Oxidation of a point defect and a grain boundary. (b) Oxidation of the dislocation lines closely perpendicular to sample surface.

oxidation patterns seen in Fig. 1: the broad and deep channels etched between grains A and B. At the same time, some of the hexagonal holes are broad but shallow. These shallow holes can be attributed to the etching of isolated point defects, like the one shown in Fig. 2a. Deeper hexagonal holes may develop when a dislocation line runs close to the normal to the sample surface, like the rightmost deep hexagon in grain B in Fig. 1. In fact this family of hexagons, aligned roughly on the same line, normal to the sample surface, corresponds to a case illustrated schematically in Fig. 2b where the axis of the etch pit changes when crossing a grain boundary parallel with the sample surface. As the grain in the topmost layer and the grain in the lower layer most frequently will have a somewhat different orientation, the edges of the hexagons etched at different depths may be rotated with respect to each other, like shown in Fig. 3a. The axis of the etch pit may shift

too, as the two vertically stacked grains may have different dislocation lines running through them, or the location of the native point defect, which will perpetuate the oxidation in the lower crystallite may not be located in the center (Fig. 3a). This scenario could be at the origin of the formation of the nested hexagonal systems of holes (see Figs. 1 and 3). Accidentally, holes with irregularly-shaped edges can also be seen (e.g., Fig. 3a). We attribute them to the presence of contaminations hindering the edge selectivity of the etching process.

The significant role of the defects in the oxidation of graphite under mild conditions together with the strong crystallographic dependence of the oxidation process may offer a promising tool to control the location of the hexagonal structures by artificially inducing defects at well-defined locations [26]. This way, pre-defined structures and networks can be created, for example: graphene nanoribbon networks, quantum dots, anti dot lattices [27–30].

Since the edges of a hexagon cut into a graphene lattice are all of the same crystallographic orientation, the hexagonal shape of the etched holes clearly indicates the strong crystallographic selectivity of our oxidation process. In fact such high degree of crystallographic selectivity has been demonstrated by us earlier for graphene layers on SiO₂ [26,31]. In that process the annealing is carried out in an oxygen free atmosphere and the oxidation proceeds with oxygen extracted from the SiO₂ substrate. The resulting edges are of zig-zag type. By contrast, with the present process we are able to provide edges of armchair orientation as evidenced by atomic resolution STM images shown in Fig. 3b. The STM image of a nested hexagonal hole-system can be seen in the Fig. 3a. The hexagons with different orientations are located in crystallites with slightly different orientation, lying on top of each other. The typical thickness of these graphite crystallites is in the range of few tens nanometers. The atomic resolution image in Fig. 3b was acquired close to the hole-edge in the third layer (marked by a black square). In the atomic resolution STM image in Fig. 3b the blue line is parallel with the edge of the etched hexagon at the same level (third layer from top). It is apparent that the type of edge is exactly of armchair orientation as also shown in the inset in the lower right corner of Fig. 3b. The upper right inset of Fig. 3b shows the Fourier transformed atomic resolution image.

The above described method provides bulk HOPG crystals with nanopatterned upper layers containing hexagons of precisely armchair oriented edges. By exfoliation of these samples it is possible to produce graphene and FLG samples with hexagonal holes of armchair edges. Fig. 4a shows a FLG with a hexagonal structure exfoliated and transferred onto Si/SiO₂ substrate. The exfoliation has been achieved by a modified thermal release tape (TRT) technique. First, we have placed the TRT on the HOPG surface, which upon tearing exfoliated a few hundreds to thousands of upper graphene layers. In this case the etched surface is in direct contact with the TR tape. Then we turned the TRT around and placed a scotch tape on the top of the exfoliated thick graphite flakes and tear the scotch tape repeatedly until, only few layer graphene flakes remained on the thermal resist tape. Afterwards we pressed strongly the thermal resist tape to the Si/SiO₂ surface and heat it up to 90 °C. The tape then released

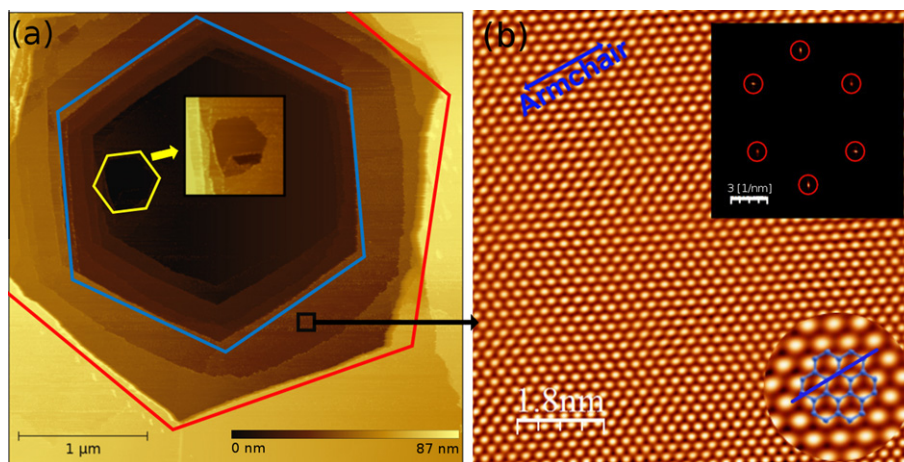


Fig. 3 – (a) STM image of an etched hexagonal hole revealing several graphite grains of different orientation (stacked on top of each other), indicated by the rotated hexagons. Inset: zoomed and lightened image of the yellow mark hole. **(b)** Atomic resolution STM image near the red hexagonal edge (marked by a black square). Upper inset: Fourier transformed atomic resolution image. The lower inset shows the armchair orientation of the lattice. (For interpretation of the references to color in this figure legend, the reader is referred to the web version of this article.)

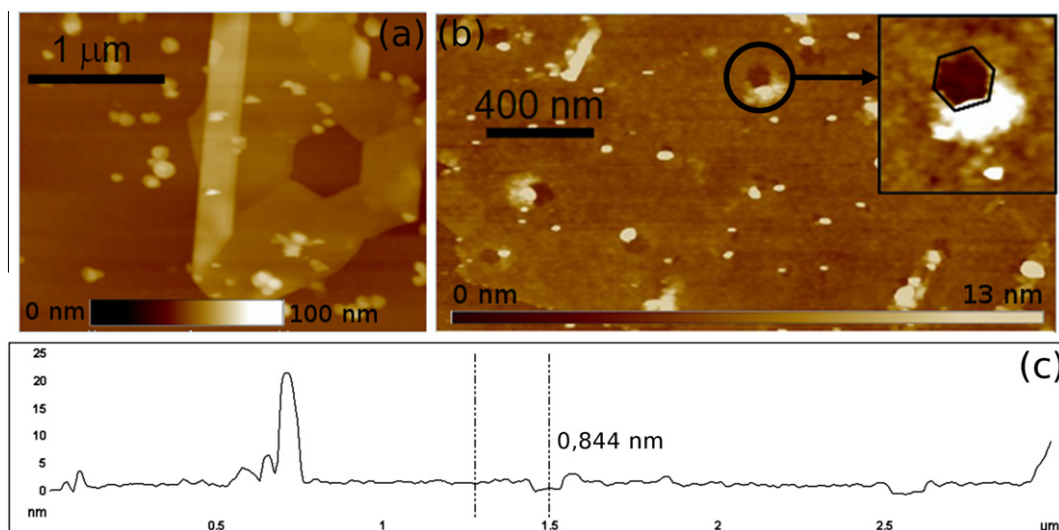


Fig. 4 – Nanopatterned FLG (a) and graphene (b) flakes transferred onto SiO₂ surface. (c) Linecut on a hexagonal hole in graphene.

the substrate, leaving graphene and FLG flakes with hexagonal holes of armchair edges (Fig. 4a). Fig. 4b shows single layer graphene flake with a 80 nm diameter armchair-edged hexagonal hole on Si/SiO₂ substrate. This sample made by the well known scotch tape method. The line cut through the hexagon shown in Fig. 4c displays an apparent height of 0.84 nm, which is in agreement with the height observed in AFM investigations of single layer graphene on SiO₂ substrates [32–34].

2.1. Discussion of the oxidation process

Fig. 5 schematically shows the basics of the graphene oxidation process, discussed in detail in the literature [35].

The oxygen atoms first bind to the carbon atoms (Fig. 5a). The oxygen molecule to be able to adsorb, must first dissociate. The binding between O and C atoms may be in plane (IP) or out of plane (OP). If the system is given enough energy (for example by heating), then carbon–carbon bonds can be broken (the electro negativity of the oxygen atoms is higher, than that of the carbon atoms). In the first step the IP oxygen will extract the C atom to which it is bound as carbon monoxide leaving the surface (Fig. 5b). In the next step, the OP oxygen atom forms a double covalent bond with the remaining carbon atom, in this way becoming an IP bond (Fig. 5c). Meanwhile, additional oxygen atoms can form OP bonds, then, the process is repeated, and the IP carbon–oxygen bond will

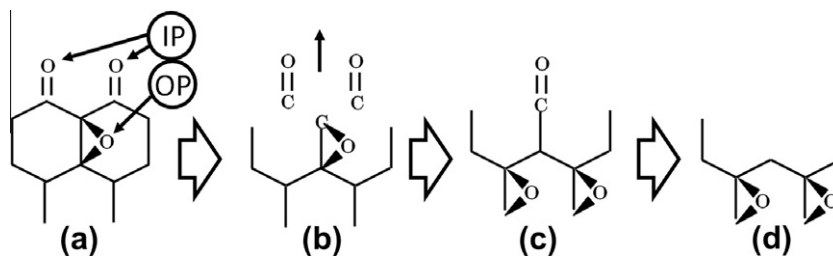


Fig. 5 – Schematic of the oxidation process.

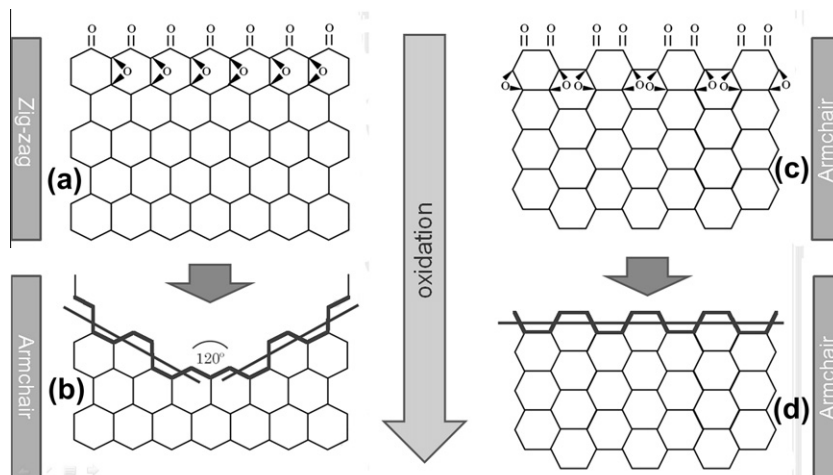


Fig. 6 – Schematics of the proposed armchair edge formation mechanism.

yield a new carbon monoxide, which leaves the surface (Fig. 5d).

As we have shown, the edges of the oxidized hexagonal holes are of armchair type. The armchair type edge formation process is a clear consequence of the above oxidation mechanism. To see this, consider a zig-zag graphene edge as starting point (Fig. 6a). When the processes detailed above, is applied step by step, the resulting edge formed by oxidation becomes armchair type as illustrated in Fig. 6b. If a similar oxidation scenario is applied starting from an armchair edge (Fig. 6c), one can observe that after the full removal of an armchair line of atoms the edge will have again an armchair termination (Fig. 6d). Consequently, if a defect with a random edge orientation is oxidized, it will rapidly evolve towards the armchair type edge, after which the orientation will be preserved. Due to the fact that the etching was carried out on surface of bulk HOPG, catalytic effects originating from the substrate can be excluded. This is in contrast with the case of etching zig-zag edges where the catalytic role of the silicon oxide substrate was shown to play an important role [26].

2.2. The effect of the oxidation parameters

We found that the size of the etched hexagons strongly depends on three particular parameters; namely, the etching temperature, the duration of the oxidation and the oxygen

concentration of the reaction atmosphere. If these parameters are precisely regulated, then not only the edge orientation but also the size of the as produced nanoarchitectures can be controlled.

In order to achieve this we have systematically measured the average diameter of the hexagonal holes while varying the different experimental parameters. We found that the diameter of the hexagonal holes (and the etched out width of the grain boundaries too) exponentially increases with increasing temperature (Fig. 7a), while keeping the other parameters constant (oxidation time of 10 min and an oxygen concentration of 30%). This exponential increase sets in at about 400 °C. Below this temperature the reaction rate tends to zero, practically no carbon-carbon bonds are affected.

We have also found a linear dependence of the hole-size with the duration of the oxidation process in experiments carried out the temperature of 650 °C and an oxygen concentration of 30%, while the duration was varied between 5 and 20 min (Fig. 7b). This finding provides an easy way to control the size of the hexagonal holes, and the nanostructures emerging in between them.

The hole size was found to linearly increase also with the oxygen concentration of the reaction atmosphere (Fig. 7c). The process was carried out in a mixture of oxygen and argon atmosphere keeping constant the total gas yield, at a temperature of 650 °C for 10 min. The oxygen content was varied between 0% and 45%.

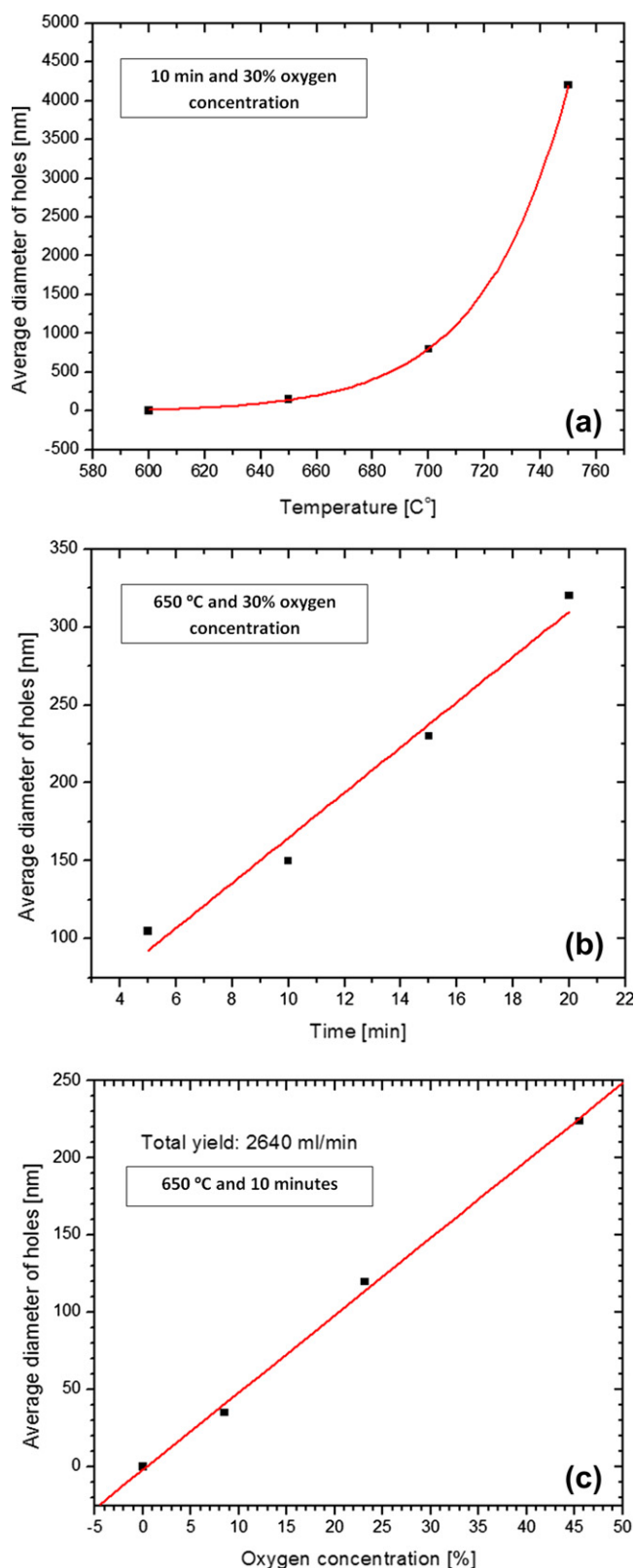


Fig. 7 – The average diameter of the hexagonal holes as a function of the etching temperature (a), duration (b), and oxygen concentration (c).

3. Conclusions

The physical properties of graphene nanoribbons and of other more complex nanostructures are strongly influenced by the crystallographic orientation of their edges. Therefore, methods that allow the production of graphene nanostructures which have edges of well defined crystallographic orientations are highly sought after. Our etching procedure presented here, is based on the controlled oxidation of graphite and offers the possibility to produce nanostructures with precisely armchair oriented edges. It is of great importance that the armchair edges are formed in a slow, well controlled process, close to chemical equilibrium. This offers a much better control over the resulting nanostructures as well as smoother edges compared to other non-equilibrium methods. The oxidation process can be well-controlled through the oxidation temperature, annealing time and the oxygen concentration. A further advantage is that the process may be used as a parallel process if a system with pre-defined defects is produced – for example by AFM indentation [26] – from which the growth of hexagonal holes will start simultaneously. This way the nanopatterning of macroscopic graphene surfaces with crystallographic orientation control can be achieved.

Additionally, the oxidation procedure described in the present paper offers a handy way for investigating the vertical stacking of graphitic crystallites in HOPG, providing information on the thickness of crystalline plates, their misorientation in the basal plane, the character and the distribution of grain boundaries, etc. This may prove useful as HOPG is one of the most widely used materials for the preparation of graphene and few layer graphite samples by various methods of mechanical and chemical exfoliation.

Acknowledgement

This work has been supported OTKA Grants K 101599 and PD 84244.

REFERENCES

- [1] Novoselov KS, Geim AK, Morozov SV, Jiang D, Zhang Y, Dubonos SV, et al. Electric field effect in atomically thin carbon films. *Science* 2004;306:666–9.
- [2] Obraztsov AN, Obraztsova EA, Tyurmina AV, Zolotukhin AA. Chemical vapor deposition of thin graphite films of nanometer thickness. *Carbon* 2007;45:2017–21.
- [3] Li X, Cai W, An J, Kim S, Nah J, Yang D, et al. Large-area synthesis of high-quality and uniform graphene films on copper foils. *Science* 2009;324:1312–4.
- [4] Wellmann R, Beottcher A, Kappes M, Kohl U, Niehus H. Growth of graphene layers on HOPG via exposure to methyl radicals. *Surf Sci* 2003;542:81–93.
- [5] Hass J, de Heer WA, Conrad EH. The growth and morphology of epitaxial multilayer graphene. *J Phys: Condens Matter* 2008;20:323202-1–323202-27.

- [6] Tung VC, Allen MJ, Yang Y, Kaner RB. High-throughput solution processing of large-scale graphene. *Nat Nanotechnol* 2009;4:25–9.
- [7] Hernandez Y, Nicolosi V, Lotya M, Blighe FM, Sun Z, De S, et al. High-yield production of graphene by liquid-phase exfoliation of graphite. *Nat Nanotechnol* 2008;3:563–8.
- [8] Castro Neto AH, Guinea F, Peres NMR, Novoselov KS, Geim AK. The electronic properties of graphene. *Rev Mod Phys* 2009;81:109–62.
- [9] Lin Y-M, Dimitrakopoulos C, Jenkins KA, Farmer DB, Chiu H-Y, Grill A, et al. 100 GHz transistors from wafer scale epitaxial graphene. *Science* 2010;327(5966):662.
- [10] Barone V, Hod O, Scuseria GE. Electronic structure and stability of semiconducting graphene nanoribbons. *Nano Lett* 2006;6(12):2748–54.
- [11] Son YW, Cohen ML, Louie SG. Energy gaps in graphene nanoribbons. *Phys Rev Lett* 2006;97:216803-1–4.
- [12] Stampfer C, Güttinger J, Hellmüller S, Molitor F, Ensslin K, Ihn T. Energy gaps in etched graphene nanoribbons. *Phys Rev Lett* 2009;102:056403-1–4.
- [13] Masubuchi S, Ono M, Yoshida K, Hirakawa K, Machida T. Fabrication of graphene nanoribbon by local anodic oxidation lithography using atomic force microscope. *Appl Phys Lett* 2009;94:082107-1–3.
- [14] Tapasztó L, Dobrik G, Lambin Ph, Biró LP. Tailoring the atomic structure of graphene nanoribbons by scanning tunneling microscope lithography. *Nat Nanotechnol* 2008;3:397–401.
- [15] Ci L, Xu Z, Wang L, Gao W, Ding F, Kelly KF, et al. Controlled nanocutting of graphene. *Nano Res* 2008;1:116–22.
- [16] Yang BR, Zhang L, Wang Y, Shi Z, Shi D, Gao H, et al. An anisotropic etching effect in the graphene basal plane. *Adv Mater* 2010;22:4014–9.
- [17] Chang H, Bard AJ. Scanning tunneling microscopy studies of carbon–oxygen reactions on highly oriented pyrolytic graphite. *J Am Chem Soc* 1991;113:5588–96.
- [18] Tandon D, Hippo EJ, Marsha H, Sebok E. Surface topography of oxidized HOPG by scanning tunneling microscopy. *Carbon* 1997;35(1):35–44.
- [19] Rodriguez-reinoso F, Thrower PA. Microscopic studies of oxidized highly oriented pyrolytic graphite. *Carbon* 1974;12(3):269–79.
- [20] Nemes-Incze P, Yoo KJ, Tapasztó L, Dobrik G, Lábár J, Horvath ZE, et al. Revealing the grain structure of graphene grown by chemical vapor deposition. *Appl Phys Lett* 2011;99(2):023104-1–3.
- [21] Kotakoski J, Meyer J. Mechanical properties of polycrystalline graphene based on a realistic atomistic model. *Phys Rev B* 2012;85:195447-1–6.
- [22] Simonis P, Goffaux C, Thiry PA, Biró LP, Lambin Ph, Meunier V. STM study of a grain boundary in graphite. *Surf Sci* 2002;511:319–22.
- [23] Lahiri J, Lin Y, Bozkurt P, Oleynik II, Batzill M. An extended defect in graphene as a metallic wire. *Nat Nanotechnol* 2010;5:326–9.
- [24] Brenner DW, Shenderova OA, Harrison JA, Stuart SJ, Ni B, Sinnott SB. A second-generation reactive empirical bond order (REBO) potential energy expression for hydrocarbons. *J Phys: Condens Matter* 2002;4:783–802.
- [25] Thrower PA, Mayer RM. Point defects and self-diffusion in graphite. *Phys Status Solidi A* 1978;47(1):11–37.
- [26] Nemes-Incze P, Magda G, Kamarás K, Biró LP. Crystallographically selective nanopatterning of graphene on SiO₂. *Nano Res* 2010;3:110–6.
- [27] Dong X, Long Q, Wang J, Chan-Park MB, Huang Y, Huang W, et al. A graphene nanoribbon network and its biosensing application. *Nanoscale* 2011;3:5156–60.
- [28] Trauzettel B, Bulaev DV, Loss D, Burkard D. Spin qubits in graphene quantum dots. *Nat Phys* 2007;3:192–6.
- [29] Ponomarenko LA, Schedin F, Katsnelson MI, Yang R, Hill EH, Novoselov KS, et al. Chaotic Dirac billiard in graphene quantum dots. *Science* 2008;320(5874):356–8.
- [30] Pedersen TG, Flindt C, Pedersen J, Mortensen NA, Jauho A-P, Pedersen K. Graphene antidot lattices: designed defects and spin qubits. *Phys Rev Lett* 2008;100(13):136804-1–4.
- [31] Krauss B, Nemes-Incze P, Skakalova V, Biró LP, von Klitzing K, Smet JH. Raman scattering at pure graphene zigzag edges. *Nano Lett* 2010;10:4544–8.
- [32] Novoselov KS, Geim AK, Morozov SV, Jiang D, Zhang Y, Dubonos V, et al. Electric field effect in atomically thin carbon films. *Science* 2004;306:666–9.
- [33] Gupta A, Chen G, Joshi P, Tadigadapa S, Eklund PC. Raman scattering from high-frequency phonons in supported *n*-graphene layer films. *Nano Lett* 2006;6:2667–73.
- [34] Nemes-Incze P, Osváth Z, Kamarás K, Biró LP. Anomalies in thickness measurements of graphene and few layer graphite crystals by tapping mode atomic force microscopy. *Carbon* 2008;46:1435–42.
- [35] Chen N, Yang RT. Ab initio molecular orbital study of the unified mechanism and pathways for gas–carbon reactions. *J Phys Chem A* 1998;102:6348–56.